Size, anisotropy and doping effects on the coercive field of ferromagnetic nanoparticles

2007 J. Phys.: Condens. Matter 19 406235

(http://iopscience.iop.org/0953-8984/19/40/406235)

IOP PUBLISHING JOURNAL OF PHYSICS: CONDENSED MATTER

J. Phys.: Condens. Matter **19** (2007) 406235 (12pp) doi:10.1088/0953-8984/19/40/406235

Size, anisotropy and doping effects on the coercive field of ferromagnetic nanoparticles

J M Wesselinowa[1] **and I Apostolova**[2]

[1] Department of Physics, University of Sofia, 5 J. Bouchier Boulevard, 1164 Sofia, Bulgaria
[2] Faculty of Forest Industry, University of Forestry, 10 Kliment Okhridsky Boulevard, 1756 Sofia, Bulgaria

Received 11 April 2007, in final form 16 August 2007
Published 21 September 2007
Online at stacks.iop.org/JPhysCM/19/406235

Abstract

The influence of size, anisotropy and doping effects on the hysteresis loop of ferromagnetic nanoparticles is studied, based on the modified Heisenberg model. A Green's function technique in real space allows the calculation of the dependence of the magnetization on the temperature, magnetic field, anisotropy, defects and particle size. It is demonstrated that the coercive field H_c is very sensitive to the surface single-ion anisotropy, and to the exchange interaction constant on the surface J_s and in the defect shells J_d. With respect to the strong surface single-site anisotropy D_s, we observe at small particle size, $N = 4$ shells, a maximum in the size dependence of the coercive field, whereas for the small surface anisotropy there is no maximum. Taking into account that J can be different in the defect shells compared to the case without defects, we have obtained for the first time that the coercive field H_c, the permanent magnetization M_r and the Curie temperature T_C can increase or decrease for different kinds of doping ions. The dependence on the particle size is discussed, too. The results are in accordance with the experimental data.

1. Introduction

Magnetic nanoparticles show a variety of unusual magnetic behaviour when compared to the bulk materials, mostly due to finite-size effects, surface/interface effects, including symmetry breaking, electronic environment/charge transfer, and magnetic interactions. For example, the Aronson Research Group [1] has recently carried out inelastic neutron scattering measurements on Co nanoparticles of 11 nm diameter. Their results indicate that the formation of a static and spontaneous magnetization within the nanoparticle only occurs below 50 K, and that the suppression from the bulk Curie temperature of Co (1388 K) is a dramatic manifestation of finite-size effects. From Moessbauer absorption spectra, Ahn *et al* [2] have reported the dependence of the average particle size on the superparamagnetic phenomena observed in cobalt ferrite nanoparticles having various sizes. The Curie temperatures increase linearly with increasing average particle size. The magnetic properties of FePt nanoparticles as a function

of particle size were studied by Christodoulides *et al* [3]. A decrease in the Curie temperature has been observed with decreasing size. The influence of nanostructure (layers and particles) on the magnetism of rare-earth materials (Gd, Dy, Tb) has been investigated [4]. The magnetic ordering temperature is reduced significantly compared to the bulk when the size is reduced below 10 nm for both the layer and the particle geometry. The Curie temperature is also related to the lattice constant. There are many experimental results which show the effects of the substitution of different ions on the phase transition temperature and the magnetic properties of nanoparticles. Co substitution for Fe enhances the Curie temperature [5, 6] whereas Mn substitution decreases T_C [7, 8]. The structure and magnetic properties of $Gd_2Co_{17-x}Al_x$ were studied by Cheng *et al* [9]. The substitution of larger Al atoms for smaller Co atoms leads to an approximately linear increase in the unit cell volumes. The saturation magnetization and the Curie temperature decrease monotonically with the increase of Al concentration. The effect of exchange interaction on spin orientation in $Nd_2(Fe_{1-x}T_x)_{14}B$, (T = Al, Si, Ti, Cr, Mn, Co, Ni and Cu) was investigated by Lin *et al* [10]. The substitution of Fe by T results in a decrease of spin reorientation temperature.

The experimental properties of the magnetic nanoparticles are strongly influenced by finite-size effects, the inherent disorder due to the variation of shapes (for example spherical, elliptical, cylindrical) and sizes of the particles in a typical assembly, and by the shape and size anisotropy as well as by interactions. The important interactions in these systems are the dipolar interactions, the short-range exchange interactions and the external magnetic field, which lead to interesting phenomena like superparamagnetism, slow relaxation times, and magnetization reversal. Moreover, surface effects such as surface anisotropy and surface exchange interaction could be important and should be taken into account in order to explain the experimental observations. The coercive field H_c is found to decrease [11–13] or to increase with decreasing particle size [14, 15]. The magnetization M_s and coercive field H_c can be improved by substitutions of La or Pr ions on Ba ion basis sites in barium hexaferrites. M_s reveals magnetic behaviour with respect to La or Pr ions content, showing an increase at first and then a decrease. H_c increases remarkably with increasing La or Pr ions content [16]. Luis *et al* have studied the magnetic properties of Co nanoparticles [17]. The effective anisotropy increases with decreasing particle's size, showing the dominant role played by surface atoms. The effect of Mn doping in FePt nanoparticles has been investigated by Tzitzios *et al* [18]. The coercivity depends on the amount of Mn added to the reaction mixture, and H_c increases significantly with the partial substitution of Pt by Mn, while the partial substitution of Fe by Mn does not affect the magnetic properties strongly. The coercive field is significantly enhanced when the nanoparticles are capped by a thin Au layer. The magnetization reversal process has been studied in ferromagnetic wires [19]. Application of a tensile stress results in an increase of the remanent magnetization and decrease of the switching field. When the tensile stress is high enough, the shape of the hysteresis loop is perfectly rectangular, which is associated with sufficiently quick reversals of magnetization.

A microscopic treatment of the magnetization of small ferromagnetic particles was developed first by Binder and co-workers using Monte Carlo techniques [20, 21]. It was shown that the magnetization near the surface of the particle is reduced. This was to be expected, because a surface spin has a smaller number of neighbours than it would have in the bulk and hence experiences a reduced mean field. The influence of shape and structure on the Curie temperature of Fe and Co nanoparticles has been investigated by Evans *et al* [22]. The magnetic properties were simulated using an atomistic approach using a classical spin Hamiltonian taking into account the long-range nature and atomic separation dependence of the exchange. The dynamic structure gives rise to a reduction in the magnetization and T_C, which is a finite-size effect to be considered beyond others such as the reduction

in coordination at the nanoparticle surface. A three-dimensional system of non-interacting magnetic nanoparticles with uniaxial anisotropies has been studied by Vargas and Laroze [23]. Equilibrium thermodynamical properties were derived by evaluating the partition function. Monte Carlo calculations were used to study the surface anisotropy effect on the coercive field [24] of small magnetic particles. Kachkachi and Dimian [25], Iglesias and Labarta [26] and Dimitrov and Wysin [27] have studied the influence of surface anisotropy on the hysteretic properties of magnetic nanoparticles. Based on Monte Carlo simulations, Yang *et al* [28] have studied the roles of the exchange (J) and dipole (D) couplings on the magnetoresistance for nanoparticles. The simulated results reveal that the coercivity H_c increases with decreasing value of D and increasing magnitude of J.

In our previous paper [29] we have analysed the influence of size and anisotropy effects on static and dynamic properties of ferromagnetic nanoparticles, such as magnetization, excitation energy and its damping. The aim of the present paper is to study the size, anisotropy and doping effects on the hysteresis loop and Curie temperature of ferromagnetic nanoparticles using a Green's function theory.

2. The model and the matrix Green's function

In this section we present the calculations to obtain the spin Green's function for a spherical ferromagnetic nanoparticle. This method seems still probably the most appropriate tool to study complex systems with low symmetry. In contrast to that for extended materials, the Green's function for small particles has to be formulated in real space. The reason for that consists of the local environment, which is the key to unravelling the properties of complex systems. Moreover, the real-space Green's function leads directly to the local density of states. This is because of the presence of, at most, only partial long-range order and, in many cases, the complete absence of global long-range order. Nevertheless, such a nanoparticle is sufficiently complex and usually involves a large number of relevant degrees of freedom. Therefore, the calculation of the real-space Green's function of such a complex system is a formidable task.

Our study is based on the Heisenberg model including single-site uniaxial anisotropy. A nanoparticle is defined by fixing the origin at a certain spin in the centre of the particle and including all spins within the particle into shells. The shells are numbered by $n = 1, \ldots, N$, where $n = 1$ denotes the central spin and $n = N$ represents the surface shell of the system; see figure 1. The surface effects are included by different coupling parameters within the surface shell and within the bulk. The spin value has been fixed to $S = 2$ for all nanoparticles, and the values of the averaged spin in the same spherical shell are assumed to be equal. The Hamiltonian of the ferromagnetic particle is given by

$$H = -\sum_{i,j} J_{ij}(S_i^+ S_j^- + S_i^z S_j^z) - \sum_i D_i (S_i^z)^2 - g\mu_B H \sum_i S_i^z, \tag{1}$$

where S_i^+, S_i^- and S_i^z are the spin operators for the localized spins at site i, J_{ij} is the exchange interaction between sites i and j, D_i ($D < 0$) is the single-site anisotropy parameter, $|D| < J$. In most experiments the anisotropy axes of the nanoparticles are most likely randomly distributed, and additionally there is a size distribution. To seperate the effects coming from the structural disorder from the temperature effects is rather difficult. Therefore, in a first step in understanding the temperature effects on the coercive field, we consider for simplicity in the present study nanoparticles all having the same spin value and the same uniaxial anisotropy energy, leaving the more complicated problem of temperature effects in a random assembly of nanoparticles to a future publication. Note that when thinking about applications a common uniaxial anisotropy axis for all particles is essential. Experimentally this challenging goal has

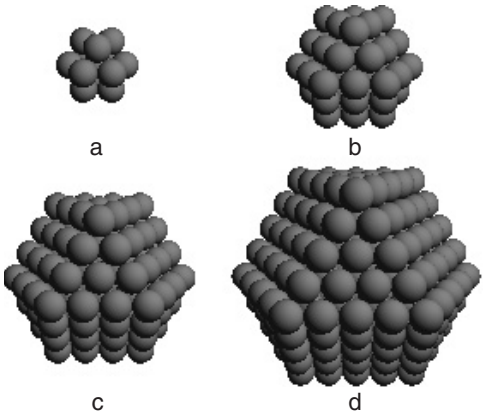

Figure 1. Array of the ferromagnetic nanoparticles composed of different shells. Each sphere represents a spin situated in the centre, and consists of one central spin $N = 1$ plus (a) 1 shell, $N = 2$, (b) 2 shells, $N = 3$, (c) 3 shells, $N = 4$, and (d) 4 shells, $N = 5$.

not been reached. If the nanoparticles are well separated, their interaction, which is of dipole type (it is of short range), is small, and will be neglected in the following. When calculations are restricted to very small nanoparticles, much smaller than the critical size to be a single domain in the remanent state, the dipolar interactions can be neglected, too. H is an external magnetic field. We assume for simplicity only nearest-neighbour exchange interaction, and take $J_{ij} = J_s$, $D_i = D_s$ on the surface of the particle and $J_{ij} = J_b$, $D_i = D_b$ in the particle. It is important to mention that the exchange interaction $J_{ij} = J(r_i - r_j)$ depends on the distance between the spins, i.e. on the lattice parameter, on the lattice symmetry and on the number of next neighbours. This is very important for investigations of ion doping effects. The Curie temperature is connected with the exchange interaction constant. The value for the isotropic Heisenberg coupling constant J can be estimated from the expression in mean-field theory [30] $J = 3k_B T_C/zS(S+1)$, where z is the number of nearest neighbours, S the spin value and k_B the Boltzmann constant. From this relation we have obtained the exchange interaction constant of bulk Fe with the body-centred cubic (bcc) lattice where $T_C = 1043$ K, $z = 8$ and $S = 2$ to be $J_b = 64, 66$ K.

To study the magnetic excitations of the magnetic particle we introduce the following Green's function:

$$G_{ij}(t) = -\mathrm{i}\theta(t)\langle[S_i^+(t), S_j^-]\rangle = \langle\langle S_i^+(t); S_j^-\rangle\rangle. \tag{2}$$

After a Fourier transformation the Green's function (2) obeys an equation of motion which in real-space representation reads

$$EG_{ij}(E) = 2\delta_{ij}\langle S_i^z\rangle + 2\sum_m J_{im}(\langle\langle S_i^+ S_m^z; S_j^-\rangle\rangle - \langle\langle S_m^+ S_i^z; S_j^-\rangle\rangle) + 2D_i\langle\langle S_i^+ S_i^z; S_j^-\rangle\rangle + g\mu_B H G_{ij}(E). \tag{3}$$

If we decouple the higher Green's function at the right-hand site of equation (3) we obtain the equation of motion in a size-dependent random phase approximation (RPA):

$$\left(E - g\mu_B H - \frac{2}{N}\sum_m J_{im}\langle S_m^z\rangle - 2D_i\langle S_i^z\rangle\right)G_{ij}(E) = 2\langle S_i^z\rangle\delta_{ij} - \frac{2\langle S_i^z\rangle}{N}\sum_m J_{im}G_{mj}(E). \tag{4}$$

The average magnetization for arbitrary magnitude of S is given by [31]

$$M = \langle S^z\rangle = \frac{1}{N'}\sum_n\left[(S+0.5)\coth[(S+0.5)\beta E_n] - 0.5\coth(0.5\beta E_n)\right], \tag{5}$$

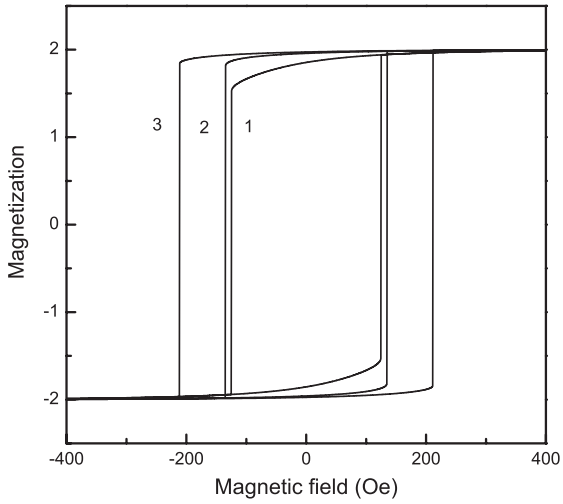

Figure 2. Magnetic field dependence of the magnetization M for $J_b = 60$ K, $D = 0$, $T = 200$ K, $N = 7$ and different J_s-values: (1) $J_s/J_b = 0.1$, (2) 1, and (3) 1.5.

where $\beta = 1/k_B T$, k_B is the Boltzman constant, and T is the absolute temperature. The elementary spin excitations of a given shell E_n can be obtained from the poles of the Green's function (3) or (4).

3. Numerical results and discussion

In this section we present the numerical results based on our theoretical calculations for a spherical cubo-octahedral ferromagnetic particle, where the following model parameters for Fe-particles are taken into account: $J_b = 60$ K, $D_b = -20$ K, $S = 2$. Due to the changed number of next neighbours on the surface or due to defects on the surface, the exchange interaction constant J can take different values on the surface, J_s, compared to the value in the particle, J_b. The value of J between the surface and the subsurface shell is J_b. We have calculated first the hysteresis loop for different values of the surface exchange interaction constant J_s, $D = 0$, $T = 200$ K, $N = \text{const}$. The results for a particle with $N = 7$ are presented in figure 2. It can be seen that both the remanence and coercivity are highly sensitive to the strength of the surface exchange interactions J_s within a nanoparticle. For the case where the exchange interaction on the surface shell has the value $J_s = 6$ K (figure 2, curve 1), i.e. $J_s < J_b$, the coercive field H_c and the remanent magnetization M_r are reduced from the values for the case where $J_s = J_b$ (curve 2). The Curie temperature T_C decreases, too, due to the smaller J_s-value. It must be here mentioned that a finite system, such as a magnetic particle, cannot show a magnetic phase transition. The magnetization curve as a function of temperature $M(T)$ does not really go to $M = 0$, but there is a characteristic 'crossover' behaviour which signals an abrupt drop of M. We choose the temperature T_C as the temperature at which $M(T)$ has the steepest slope (and which can be seen as a finite-system analogue of the Curie temperature T_C). For the case where $J_s = 90$ K (figure 2, curve 3), i.e. $J_s > J_b$, H_c and M_r are enhanced compared to the case for $J_s = J_b$ (curve 2). T_C of the small particle is raised due to the presence of larger J_s-values. This is the opposite behaviour compared to the case of $J_s < J_b$. Polesya *et al* [32] have studied the magnetic properties of free Fe clusters at finite temperatures from first principles, and have found that T_C is not a monotonic function of the cluster size. Figure 3 shows the temperature

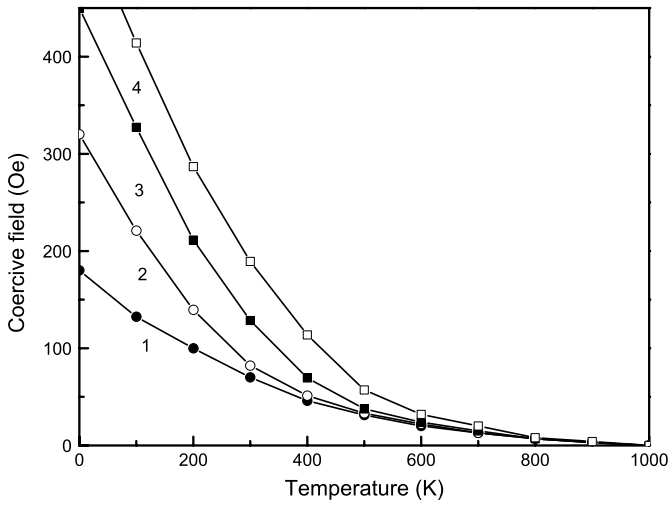

Figure 3. Temperature dependence of the coercive field H_c for $J_b = 60$ K, $D = 0$, $N = 7$ and different J_s-values: (1) $J_s/J_b = 0.5$, (2) 1, (3) 1.5, and (4) 2.

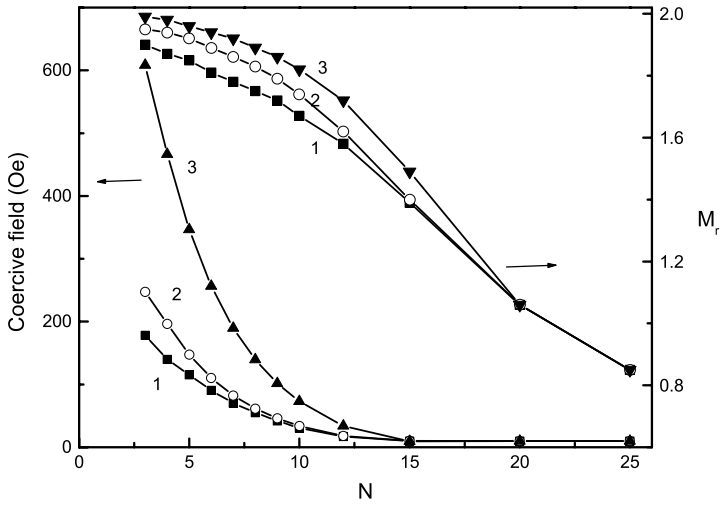

Figure 4. Particle size dependence of the coercive field H_c and the remanent polarization M_r for $J_b = 60$ K, $D = 0$, $T = 300$ K and different J_s-values: (1) $J_s/J_b = 0.2$, (2) 1, and (3) 2.

dependence of the coercive field for $N = 7$. It can be seen that H_c has its largest value at low temperatures and it decreases as the temperature approaches the Curie temperature T_C, where a paramagnetic behaviour is expected. The coercive field decreases with increasing of $T \to T_C$ for both cases $J_s < J_b$ and $J_s > J_b$, and this can be explained by the thermal disorder at higher temperatures. This is in agreement with many experimental data [33–36].

Moreover, we have investigated the dependence of the remanent magnetization M_r and the coercive field H_c on their particle size N. H_c and M_r of magnetic nanoparticles can be changed by controlling their size. The results are shown in figure 4. M_r and H_c increase with decreasing N for both cases $J_s < J_b$ and $J_s > J_b$, which is in accordance with theoretical [13, 24–26] and experimental data from different magnetic particles [14, 15, 34, 37]. It is known that very

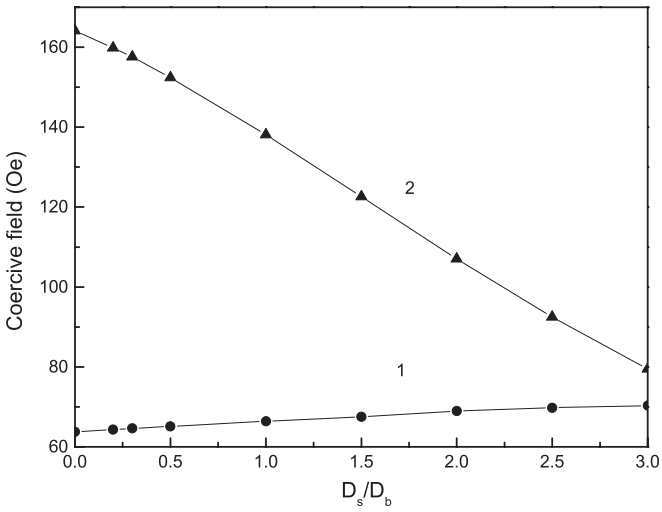

Figure 5. Anisotropy dependence of the coercive field H_c for $J_b = 60$ K, $T = 300$ K, $N = 7$ and different J_s-values: (1) $J_s/J_b = 0.2$, and (2) 2.

small particles are superparamagnetic even at low temperatures, and there is no hysteresis. In our calculations, this is the case for $N < 3$.

In the previous calculations we have neglected the effects of the anisotropy. There is some experimental evidence that the magnetic anisotropy of nanoparticles can be larger [38, 39] or smaller [40, 41] than that of the bulk materials. A major contribution of this enhancement or reduction comes from the surface spins. Figure 5 shows the influence of the single-ion anisotropy constant D on the size dependence of the coercive field. It can be seen that H_c can increase (figure 4, curve 1) or decrease (figure 5, curve 2) for different J_s-values and D_s-values, which is in agreement with the experimental data. The coercive field H_c is found to decrease [11–13] or to increase with decreasing particle size [14, 15]. There is some competition effect between J_s and D_s. In the case of $J_s < J_b$, an increase of D_s enhances H_c, whereas for $J_s > J_b$, with raising of D_s, H_c is reduced. As the volumes of the magnetic particles have shrunk to reach recording densities of the order of 100 Gb/in^2 T or more, materials with higher coercivities due to strong crystalline anisotropies have been employed. Taking into account the magnetic anisotropy for the case $J_s < J_b$ and $D_s \geqslant D_b$ we obtain that for small particle size ($N < 3$) the coercive field is zero, then with increase of particle size H_c passes trough a maximum at a critical size ($N_{cr} = 4$ for these model parameters) (figure 6). The maximum value is temperature dependent: it decreases strongly with increasing temperature. We speculate that the transition of a single-domain structure to a multi-domain structure in our particle depends on the temperature. As a result, the magnetic coercivity decreases with decreasing particle size for particles below the superparamagnetic size limit. The limit appears as a maximum in a curve showing switching field or coercivity versus particle size, such as in figure 6. This behaviour is in good agreement with that expected for small particles and is related to the existence of different magnetic processes in the particles [42]. Such a maximum in H_c at diameters of ≈10–20 nm is obtained experimentally due to strong surface anisotropy, for example in spherical particles of Fe and Co [43], Fe, Co, and Ni ultrafine particles [44], spherical Co–Ni and Fe–Co–Ni particles [45], carbon-encapsulated Co particles [46], yttrium iron garnet nanoparticles [42], rare-earth (Gd, Dy, Tb) nanoparticles [4], $CoFe_2O_4$ nanoparticles [47] and $NiFe_2O_4$ nanoparticles [48]. We can

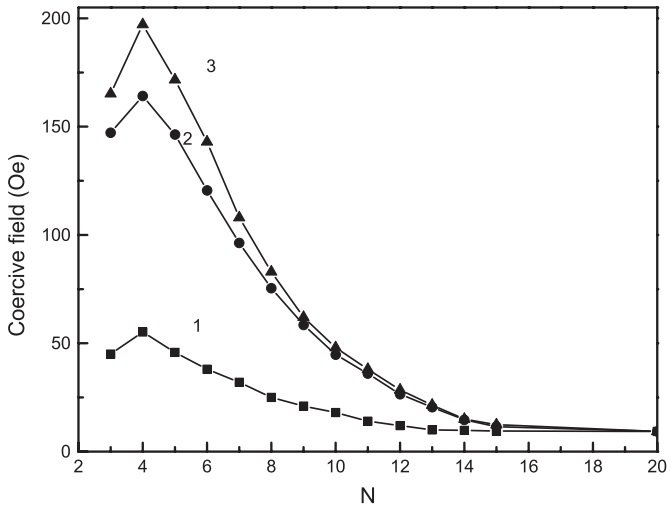

Figure 6. Particle size dependence of the coercive field H_c for $J_s/J_b = 0.2$, $D_b = -20$ K and different D_s-values and T-values: (1) $D_s/D_b = 3$, $T = 600$ K, (2) $D_s/D_b = 0.2$, $T = 200$ K, and (3) $D_s/D_b = 3$, $T = 200$ K.

conclude that the magnetic anisotropy plays a dominant role in determining the magnetic properties of small particles and must be taken into account in order to explain the experimental data.

In order to study the doping effects on the hysteresis loop we assume additionally that one or more of the shells can be defected. The interaction strength of these defect shells is characterized by J_d. The interaction constant between a defected and nondefected shell is J_b. Let us first consider the case where in a particle with $N = 7$ we have a defective central atom plus four shells, i.e. from $n = 1$ to 5. For example, this can be originated by localized vacancies or impurities, doping ions with smaller radii and larger distances between them in comparison to the host material. It is reasonable to assume that the exchange interaction $J_d(r_i - r_j)$, which depends on the distance between the neighbouring spins, is smaller than the value of the interaction for the case without defects $J_b = 60$ K, and has a value in the defect shells for example $J_d = 30$ K (compare figure 7, curve 1). The coercive field and the remanent magnetization are smaller than in the case without defects, $J_d = J_b$ (figure 7, curve 2). This case, where $J_d < J_b$, could explain the experimentally obtained decrease of H_c and M_r in ferromagnetic small particles by substitution of doping ions, such as Cr in $SrFe_{12-x}Cr_xO_{19}$ nanoparticles [49], Cu in Fe–Si–B ultrafine grain structure and tin-doped ferrite particles [11]. For the case where $J_d = 90$ K (figure 7, curve 3), i.e. J_d is larger than the value without defects J_b (for example when the impurities have a larger radius compared with the constituent ions), the coercive field, the remanent magnetization and the Curie temperature are larger than for the case without defects, $J_d = J_b$ (figure 7, curve 2). The quantities of the particle are enhanced in comparison to the value without defects due to the presence of larger J_d-values. This is the opposite behaviour compared to the case of $J_d = 30$ K, $J_d < J_b$. The second case, where $J_d > J_b$, could explain the experimentally obtained increase in H_c and M_r by the substitution of doping ions, such as Pt in Fe–Pt [50], rare earths (Nd, Sm, Eu, Tb) in Fe nanoparticles [51], Pr in Pr–Fe–B-type [52] nanocomposite magnets.

From figure 7 one can observe that the coercive field, the remanent magnetization and the Curie temperature of the magnetic particle are decreased or increased due to different

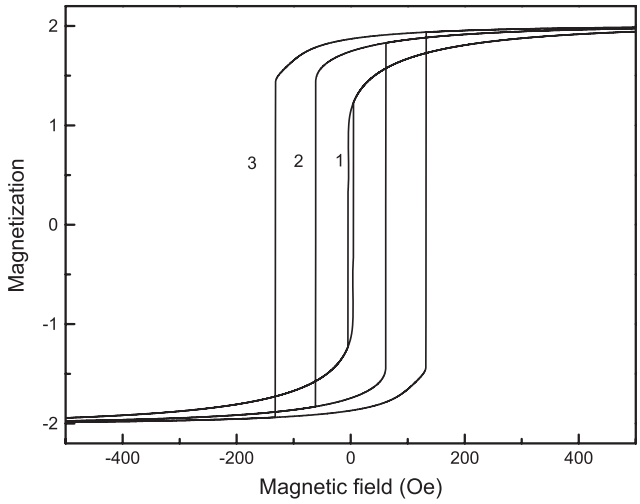

Figure 7. Magnetic field dependence of the magnetization M for $J_s/J_b = 0.5$, $D_s/D_b = 1$, $T = 300$ K, $N = 7$ and different J_d-values: (1) $J_d/J_b = 0.5$, (2) 1, and (3) 1.5.

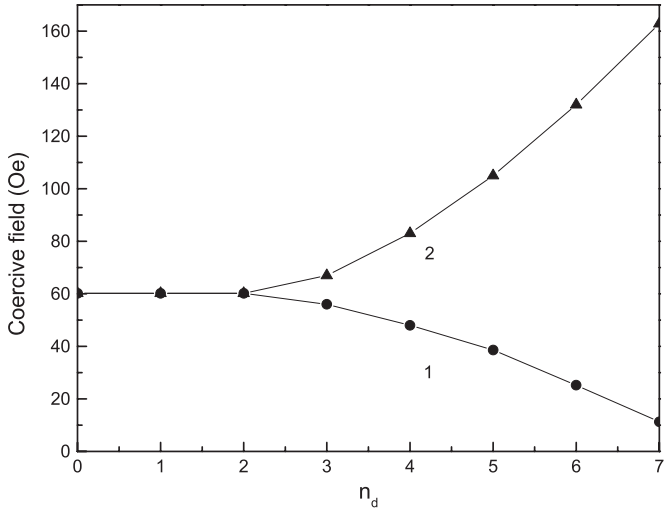

Figure 8. Dependence of the coercive field H_c on the number of defected shells for $J_s/J_b = 0.5$, $D_s/D_b = 1$, $N = 7$, $T = 300$ K and different J_d-values: (1) $J_d/J_b = 0.5$, and (2) 1.5.

exchange interactions in the defect shells. H_c, M_r and T_C are dependent, too, on how many inner shells are defected, i.e. they are dependent on the concentration of the defects. This is demonstrated in figures 8 and 9 for a particle with $N = 7$. It can be seen that for $J_s = \text{const}$, $D_s = \text{const}$ and $J_d = 30$ K, i.e. $J_d < J_b$, with increasing number of defect shells $n_d H_c$ (respectively M_r) decreases (figure 8, curve 1), ($n_d = 0$ means no defects, $n_d = 1$ we have one defective shell (a defective central atom), $n_d = 2$ we have two defective shells (a defective central atom + defective 1 shell) and so on). This is in reasonable accordance with the experimental data of Mohapatra *et al* [54] and Cheng *et al* [9], who have studied the influence of Ni doping on the properties of fine magnetite particles and the Al substitution on Gd_2Co_{17} nanoparticles, respectively. The coercive field decreases with the presence of Ni in

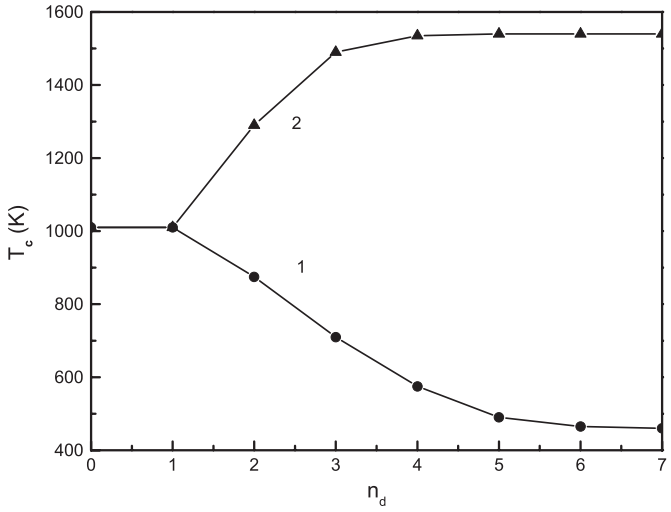

Figure 9. Dependence of the critical temperature T_C on the number of defected shells for $J_s/J_b = 0.5$, $D_s/D_b = 1$, $N = 7$ and different J_d-values: (1) $J_d/J_b = 0.5$, (2) 1.5.

magnetite nanoparticles [54] and Cr in FePt nanoparticles [55]. The opposite behaviour can be obtained for $J_d = 90$ K, i.e. $J_d > J_b$ (figure 8, curve 2). With an increase of the number of defect shells H_c (respectively M_r) increases. This is in good agreement with the experimental data of Varanda *et al* [51] that the coercive field increases with the rare-earth composition in $Fe_{1-x}RE_x$, RE = Nd, Sm, Eu, Tb. If we start first with a defective surface shell, then add a defective subsurface shell and so on, we obtain a similar dependence of H_c as in figure 7, but the decrease or increase of H_c begins at $n_d = 3$.

T_C is found to be also dependent on the value of the exchange interaction constant in the defect shells J_d, i.e. on the radius of the defect ion as well as on the ion doping concentration. Figure 9 shows the dependence of the Curie temperature T_C on the number of defect shells n_d for a spherical particle with $N = 7$ for different J_d-values. We find that the size-dependent Curie temperatures of the ferromagnetic particle are increased or decreased due to different exchange interactions in the defect shells. For the realization $J_d < J_b$ the Curie temperature T_C decreases with increasing number of defect shells (figure 9, curve 1). The denotation of n_d is the same as in figure 8. This is in reasonable accordance with the experimental data of Mohapatra *et al* [54] and Cheng *et al* [9], who have studied the influence of Ni doping on the properties of fine magnetite particles and the Al substitution on Gd_2Co_{17} nanoparticles, respectively. The Mn substitution for Fe decreases T_C, too [7, 8]. The substitution of larger Al atoms for smaller Co atoms (or Ni atoms for smaller Fe atoms) leads to an approximately linear increase in the unit cell volumes and a monotonic decrease of T_C. Since the Co–Co exchange coupling constants are about one order of magnitude larger than the Al–Co exchange coupling constants, the Curie temperature in Co-rich compounds is mainly determined by the direct Co–Co exchange interactions. The fact that the Curie temperature decreases monotonically with increasing Co–Co interatomic distance suggests that the increase of Co–Co distance leads to a decrease of the Co–Co exchange interactions. This would corresponds in our case to $J_d < J_b$. For the other case, $J_d > J_b$, we obtain an increase of T_C with increasing number of defect shells. This case could explain the experimental data of Chang *et al* [5] and Zhang *et al* [6], who have found that Co substitution in $Nd_2Fe_{14}B$ and $Pr_9Fe_{85}B_5$ nanocomposites improves the Curie temperature. A Cu capping layer induces an enhancement of T_C in both

Fe and Co magnetic nanoparticle assemblies [53]. The proper doping amount of magnetic Gd ion can enlarge the saturation magnetization M_s, T_C and coercive field H_c of $CoFe_2O_4$ nanocrystalline films, whereas the doping of Y reduces them [56]. Recently, Narayan [57] has studied the critical size for defects in nanostructured materials. It was found that, as the grain size is reduced, there is a critical size below which the defect can be reduced virtually to zero. This critical size for most defects in solid-state materials falls in the nanoscale regime. Thus, nanostructured materials offer a unique opportunity to realize the property of a perfect material.

4. Conclusions

Using a modified Heisenberg model and a Green's function technique we have calculated the dependence of the magnetization of ferromagnetic nanoparticles on the temperature, magnetic field, anisotropy, defects and particle size. The particles all have the same uniaxial anisotropy axis with static applied magnetic field parallel to this axis. We have shown that the surface single-site anisotropy D_s plays a dominant role in determining the magnetic properties of particles and that it must be taken into account in order to explain the experimental data, for example the obtained maximum in the particle size dependence of the coercive field $H_c(N)$. The maximum value is temperature dependent: it decreases strongly with increasing temperature. Moreover, H_c can increase or decrease with N for different surface exchange interaction J_s and surface anisotropy D_s. There is some competition effect between J_s and D_s. It must be noted that H_c also depends strongly on the shape of the particles, especially for elliptical nanoparticles. The shape dependence will be discussed in a forthcoming paper. We have studied for the first time theoretically the influence of different ion doping on the coercive field. H_c is very sensitive to the exchange interaction constant in the defect shell, J_d. For J_d smaller than the value without defects, $J_d < J_b$ (for example when the impurities have a smaller radius compared with the constituent ions), the coercive field H_c, the remanent magnetization M_r, and the Curie temperature T_C are smaller than for the case without defects, whereas for the case $J_d > J_b$ H_c, M_r and T_C are larger than for the case without defects. The results are in qualitative agreement with the experimental data.

References

[1] Aronson M, private communication, University of Michigan
[2] Ahn Y, Choi E J and Kim E H 2003 *Rev. Adv. Mater. Sci.* **5** 477
[3] Christodoulides J A, Bonder M J, Huang Y, Zhang Y, Stoyanov S and Hadjipanayis G C 2003 *Phys. Rev.* B **68** 054428
[4] O'Shea M J and Perera P 1999 *J. Appl. Phys.* **85** 4322
[5] Chang W C, Wu S H, Ma B M, Bounds C O and Yao S Y 1998 *J. Appl. Phys.* **83** 2147
[6] Zhang W, Yan A, Zhang H and Shen B 2001 *J. Alloys Compounds* **315** 174
[7] Saravanan P, Alam S, Kandpal L D and Mathur G N 2002 *J. Mater. Sci. Lett.* **21** 1135
[8] Luo J, Liang J K, Liu Q L, Liu F S, Zhang Y, Sun B J and Rao G H 2005 *J. Appl. Phys.* **97** 086106
[9] Cheng Z, Shen B, Zhang J, Liang B, Guo H and Kronmueller H 1997 *Appl. Phys. Lett.* **70** 3467
[10] Lin C, Liu Z X, Sun Y X, Bai C X and Zhao T S 1989 *Phys. Rev.* B **39** 7273
[11] Liu F, Li T and Zheng H 2004 *Phys. Lett.* A **323** 305
[12] Lin C, Chiang R, Wang J and Sung T 2006 *J. Appl. Phys.* **99** 08N710
[13] Goya G F, Berquo T S, Fonseca F C and Morales M P 2003 *J. Appl. Phys.* **94** 3520
[14] Lee Y, Lee J, Bae C J, Park J G, Noh H J, Park J H and Hzeon T 2005 *Adv. Funct. Mater.* **15** 503
[15] Zhang Z, Chen X, Zhang X and Shi C 2006 *Solid State Commun.* **139** 403
[16] Ounnunkad S 2006 *Solid State Commun.* **138** 472
[17] Luis F, Bartolome J, Bartolome F, Martinez M J, Garcia L M, Petroff F, Deranlot C, Wilhelm F and Rogalev A 2006 *J. Appl. Phys.* **99** 08G705
[18] Tzitzios V, Basina G, Gjoka M, Niarchos D, Devin E and Petridis D 2006 *Nanotechnology* **17** 4270

[19] Chizhik A, Garcia C, Gawronski P, Zhukov A, Gonzalez J, Blanco J M and Kulakowski K 2005 *J. Magn. Magn. Mater.* **294** e167
[20] Binder K, Rauch H and Wildpaner V 1970 *J. Phys. Chem. Solids* **31** 391
[21] Binder K 1972 *Physica* **62** 508
[22] Evans R, Nowak U, Dorfbauer F, Shrefl T, Mryasov O, Chantrell R W and Grochola G 2006 *J. Appl. Phys.* **99** 08G703
[23] Vargas P and Laroze D 2004 *J. Magn. Magn. Mater.* **272** e1345
[24] Zianni X, Trohidou K N and Blackman J A 1997 *J. Appl. Phys.* **81** 4739
[25] Kachkachi H and Dimian M 2002 *Phys. Rev.* B **66** 174419
[26] Iglesias O and Labarta A 2005 *J. Magn. Magn. Mater.* **290/291** 738
[27] Dimitrov D A and Wysin G M 1994 *Phys. Rev.* B **50** 3077
[28] Yang Y, Shen S, Ye Q, Lin L and Huang Z 2006 *J. Magn. Magn. Mater.* **303** e312
[29] Wesselinowa J M and Apostolova I 2007 *J. Phys.: Condens. Matter* **19** 216208
[30] Ashcroft N W and Mermin N D 1976 *Solid State Physics* (New York: Holt, Rinehart and Winston)
[31] Korecki J, Przybylski M and Gradmann U 1990 *J. Magn. Magn. Mater.* **89** 325
[32] Polesya S, Sipr O, Bornmann S, Minar J and Ebert H 2006 *Europhys. Lett.* **74** 1074
[33] Gangopadhyay S, Hadjipanayis G C, Dale B, Sorensen C M, Klabunde K J, Papaefthymiou V and Kostikas A 1992 *Phys. Rev.* B **45** 9778
[34] Luna C 2003 *Nanotechnology* **14** 268
[35] Graf C P, Birringer R and Michels A 2006 *Phys. Rev.* B **73** 212401
[36] Zysler R D, Mansilla M V and Fiorani D 2004 *Eur. Phys. J.* B **41** 171
[37] Huang Y, Zhang Y, Hadjipanayis G C, Simopoulos A and Weller D 2002 *IEEE Trans. Magn.* **38** 2604
[38] Respaud M, Broto J M, Rakoto H, Fert A R, Thomas L, Barbara B, Verelst M, Snoeck E, Lecante P, Mosset A, Osuna J, Ould Ely T, Amiens C, Chaudret B, Xie Y and Blackmann J A 2004 *J. Phys.: Condens. Matter* **16** 3163
[39] Chunder S, Kumar S, Krishnamurthy A, Srivastava B K and Aswal V K 2003 *Pramana J. Phys.* **61** 617
[40] Fernandez C de J, Mattei G, Maurizio C, Cattaruzza E, Padovani S, Battaglin G, Gonella F, D'Acapito F and Mazzoldi P 2005 *J. Magn. Magn. Mater.* **290/291** 187
[41] Sharma V K and Baiker A 1981 *J. Chem. Phys.* **75** 5596
[42] Sanchez R D, Rivas J, Vaqueiro P, Lopez-Quintela M A and Caeiro D 2002 *J. Magn. Magn. Mater.* **247** 92
[43] Kneller E F and Lubersky F E 1963 *J. Appl. Phys.* **63** 656
[44] Gong W, Li H, Zhao Z and Chen J 1991 *J. Appl. Phys.* **69** 5119
[45] Mercier D, Levy J-C S, Viau G, Fievet-Vincent F, Fievet F, Toneguezzo P and Acher O 2000 *Phys. Rev.* B **62** 532
[46] Bonard J-M, Seraphin S, Beeli C, Wegrowe J-E, Stoeckli T, Jiao J, Stadelmann P A and Chatelain A 1998 *Recent Advances in the Chemistry and Physics of Fullerenes and Related Materials* vol 6, ed K M Kadish and R S Rurff (Pennington, NJ: The Electrochemical Society)
[47] Maaz K, Mumtaz A, Hasanain S K and Ceylon A 2007 *J. Magn. Magn. Mater.* **308** 289
[48] George M, John A M, Nair S S, Joy P A and Anantharaman M R 2006 *J. Magn. Magn. Mater.* **302** 190
[49] Fang Q, Cheng H, Huang K, Wang J, Li R and Jiao Y 2005 *J. Magn. Magn. Mater.* **294** 281
[50] Kawai K, Honda S, Sugiki R, Komatsu M and Kawabata K 2005 *J. Magn. Magn. Mater.* **287** 214
[51] Varanda L C, Morales M P, Goya G F, Imaizumi M, Serna C J and Jafelicci M Jr 2004 *Mater. Sci. Eng.* **112** 188
[52] You C Y, Ping D H and Hono K 2006 *J. Magn. Magn. Mater.* **299** 136
[53] Lin W, Huang P, Song K and Lin M 2006 *Appl. Phys. Lett.* **88** 153117
[54] Mohapatra M, Pandey B, Upadhyay C, Anand S, Das R P and Verma H C 2005 *J. Magn. Magn. Mater.* **295** 44
[55] Srivastava C, Thompson G B, Harell J W and Nikles D E 2006 *J. Appl. Phys.* **99** 054304
[56] Yan C, Cheng F, Peng Z, Xu Z and Liao C 1998 *J. Appl. Phys.* **84** 5703
[57] Narayan J 2006 *J. Appl. Phys.* **100** 034309